Exciton Diffusion and Annihilation in Nanophotonic Purcell Landscapes

ADVANCED OPTICAL MATERIALS
www.advopticalmat.de

Exciton Diffusion and Annihilation in Nanophotonic Purcell Landscapes

*T. V. Raziman, C. Peter Visser, Shaojun Wang, Jaime Gómez Rivas, and Alberto G. Curto**

Excitons spread through diffusion and interact through exciton–exciton annihilation. Nanophotonics can counteract the resulting decrease in light emission. However, conventional enhancement treats emitters as immobile and non-interacting. It neglects exciton redistribution between regions with different enhancements and the increase in non-radiative decay at high exciton densities. Here, the authors went beyond the localized Purcell effect to exploit exciton dynamics and turn their typically detrimental impact into additional emission. As interacting excitons diffuse through optical hotspots, the balance of excitonic and nanophotonic properties leads to either enhanced or suppressed photoluminescence. The dominant enhancement mechanisms are identified in the limits of high and low diffusion and annihilation. Diffusion lifts the requirement of spatial overlap between excitation and emission enhancements, which are harnessed to maximize emission from highly diffusive excitons. In the presence of annihilation, improved enhancement is predicted at increasing powers in nanophotonic systems dominated by emission enhancement. The guidelines are relevant for efficient and high-power light-emitting diodes and lasers tailored to the rich dynamics of excitonic materials such as monolayer semiconductors, perovskites, or organic crystals.

1. Introduction

Nanophotonics can improve light emission by enhancing excitation and radiative rates, and beaming radiation.[1–13] In the conventional Purcell effect, emitters such as molecules and quantum dots are treated as localized point dipoles.[14,15] Total enhancement thus benefits from the product of excitation and emission at a point, which guides the design of nanoresonators and metamaterials made of metals and dielectrics.

For excitonic emitters, however, the picture of emission arising from non-interacting dipoles at fixed positions is incomplete. In a variety of semiconductors, excitons are mobile and spread to large diffusion lengths compared to nanophotonic scales (10–500 nm). Examples include perovskites (diffusion length $L_D \approx$ 100–1000 nm),[16–18] monolayer transition metal dichalcogenides (hundreds of nm),[19,20] quantum dots (tens of nm),[21,22] organic crystals (1–100 nm for singlet excitons, 10–1000 nm for triplets),[23] and carbon nanotubes (hundreds of nm).[24,25] As a result, excitons can emit far from the intense near field where they originate, affecting their radiative rate. Additionally, diffusion deteriorates emission as emitters approach defects and boundaries, where they might decay non-radiatively.[26–29] A photonic modification of the radiative decay rate could decrease the effective diffusion length, thus improving performance.

Another important aspect of exciton dynamics is exciton–exciton annihilation.[25,30,31] At high exciton densities, this nonlinear process contributes to and even dominates non-radiative losses, degrading the performance of light-emitting devices at high powers,[32,33] and potentially preventing lasing. Annihilation thus curtails the advantages of nanophotonic intensity enhancement as well by simultaneously increasing non-radiative decay.

Here, we analyze the interplay of exciton dynamics and nanophotonic enhancement for thin films of excitonic emitters in nanostructured landscapes. We provide analytical results for enhancement under limiting cases of exciton dynamics. We demonstrate that, although diffusion and annihilation typically impede nanophotonic enhancement, it is possible to design nanostructures to overcome the lost efficiency. Diffusion can increase photoluminescence by taking excitons to highly radiative locations when excitation and emission are spatially decoupled. Radiative rate enhancement can ameliorate the loss of efficiency arising from annihilation, while the interplay between annihilation and diffusion can improve performance by redistributing the local exciton density. In summary,

T. V. Raziman, C. P. Visser, S. Wang, J. Gómez Rivas, A. G. Curto
Department of Applied Physics and Institute for Photonic Integration
Eindhoven University of Technology
Eindhoven 5600 MB, The Netherlands
E-mail: a.g.curto@tue.nl

S. Wang
MOE Key Laboratory of Modern Optical Technologies and Jiangsu Key Laboratory of Advanced Optical Manufacturing Technologies
School of Optoelectronic Science and Engineering
Soochow University
Suzhou 215006, China

The ORCID identification number(s) for the author(s) of this article can be found under https://doi.org/10.1002/adom.202200103.

DOI: 10.1002/adom.202200103

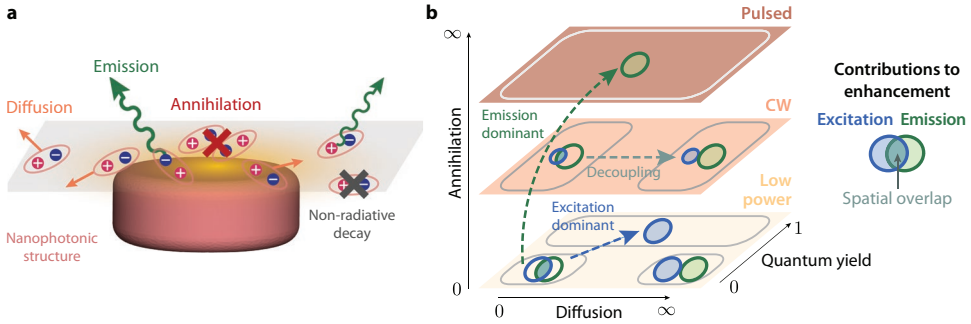

Figure 1. Impact of exciton dynamics on nanophotonic emission enhancement. a) Excitation and emission of a thin excitonic film (gray) above an array of nanodisks in the presence of diffusion and annihilation. Excitation enhancement (orange cloud) generates excitons that diffuse (orange arrows), annihilate (red), or decay non-radiatively (black) before radiative decay (green). b) Contributions to the total photoluminescence enhancement of excitation, emission, and their spatial overlap (see Table 1). Limiting cases of diffusion, annihilation, and quantum yield with qualitatively similar enhancement behaviors are grouped into common areas. At low power, diffusion lifts the requirement of spatial overlap between excitation and emission enhancements for emitters with low quantum yield, whereas enhancement with high quantum yield is independent of diffusion or emission enhancement. At high power, the benefit of excitation enhancement decreases and even vanishes for continuous-wave and pulsed illuminations, with emission dominating the total enhancement. For continuous-wave illumination, enhancement depends on diffusion but is independent of quantum yield; for pulsed illumination, enhancement does not depend on quantum yield or diffusion.

a careful balance of the relative strengths and spatial overlap of excitation and emission enhancements is the key to efficient excitonic-nanophotonic systems. Our guidelines for tailoring nanophotonic structures to diffusing and annihilating excitons will aid the design of efficient light-emitting devices.

2. Results

2.1. Exciton Dynamics and Nanophotonic Enhancement

Excitons evolve in nanophotonic environments under the combined influence of incident intensity, radiative enhancement, non-radiative decay, diffusion, and annihilation (**Figure 1**a). We consider excitonic emitters in ultrathin films on top of nanodisk arrays with a negligible variation of electromagnetic fields across the film thickness. The 2D exciton density evolves according to the exciton dynamics equation[20]

$$\frac{\partial n(\mathbf{r},t)}{\partial t} = I(\mathbf{r},t)\sigma - \left[\Gamma_r(\mathbf{r}) + \Gamma_{\mathrm{nr},0}\right] n(\mathbf{r},t) + D\nabla^2 n(\mathbf{r},t) - \gamma n^2(\mathbf{r},t) \quad (1)$$

where $n(\mathbf{r},t)$ is the exciton density at point $\mathbf{r}$ at time t, I is the nanophotonically enhanced local excitation intensity of at $\mathbf{r}$, σ is the absorption coefficient, $\Gamma_r(\mathbf{r})$ is the spatially varying radiative decay rate, $\Gamma_{\mathrm{nr},0}$ is the intrinsic non-radiative decay rate, D is the diffusion constant, and γ is the annihilation constant. In the absence of nanophotonic structures, the intrinsic decay rates are $\Gamma_{r,0} = \eta_0\Gamma_0$ and $\Gamma_{\mathrm{nr},0} = (1-\eta_0)\Gamma_0$, where Γ_0 is the total decay rate and η_0 is the intrinsic quantum yield. The exciton decay time is $\tau_0 = 1/\Gamma_0$ and the diffusion length is $L_D = \sqrt{D\tau_0}$. We assume that the nanostructures do not modify the non-radiative decay rate $\Gamma_{\mathrm{nr},0}$ and the diffusion constant D, although our model can incorporate such changes as well. We also neglect saturation of absorption at high power.

To compare systems with different excitonic and nanophotonic properties and extract the universal behavior of nanophotonic systems in the presence of exciton dynamics, we non-dimensionalize Equation (1). We identify physically relevant scales of exciton density, incident power, length, and time in the system to scale the variables n, I, $\mathbf{r}$, and t with these values:

- $n' = n/n_0$, where $n_0 = \Gamma_0/\gamma$ is the exciton density at which $\Gamma_0 n$ (the intrinsic total decay, which includes radiative and non-radiative rates but not annihilation) equals γn^2 (the density-dependent annihilation),
- $I' = I/I_0$, where $I_0 = \Gamma_0 n_0/\sigma$ is the incident continuous-wave power at which $I\sigma$ (the exciton generation) equals $\Gamma_0 n_0$ (the intrinsic decay at $n = n_0$),
- $\mathbf{r}' = \mathbf{r}/P$, where P is the period of the nanophotonic structures,
- $t' = t/\tau_0$, where τ_0 is the exciton decay time.

The characteristic scales depend on both excitonic and nanophotonic properties. Note that we perform scaling with respect to intrinsic properties (in the absence of nanostructures), except the length scale, which is the period of the array. Expressing Equation (1) in terms of the primed variables, we obtain the non-dimensionalized exciton dynamics equation

$$\frac{\partial n'(\mathbf{r}',t')}{\partial t'} = F_{\mathrm{ex}}(\mathbf{r}')I'(t') - F_{\mathrm{decay}}(\mathbf{r}',\eta_0)n'(\mathbf{r}',t') + D'\nabla'^2 n'(\mathbf{r}',t') - n'^2(\mathbf{r}',t') \quad (2)$$

where F_{ex} and F_{em} are the local nanophotonic excitation and radiative rate enhancements, and $F_{\mathrm{decay}} = \eta_0 F_{\mathrm{em}} + 1 - \eta_0$ is the localized total decay rate enhancement. The non-dimensionalized diffusion constant $D' = D\tau_0/P^2$ is related to the diffusion length and the period of the nanophotonic structures by $D' = (L_D/P)^2$. The annihilation rate γ does not appear explicitly and is part of the characteristic incident power $I' = I\gamma\sigma/\Gamma_0^2$, demonstrating the utility of non-dimensionalization in comparing different systems. Excitonic materials that differ only in the annihilation rate γ will behave identically in a nanophotonic system except for scaling of incident power. We perform electromagnetic simulations using the surface integral equation (SIE) method and solve the non-dimensionalized exciton dynamics Equation (2) to demonstrate the impact of exciton diffusion and annihilation on nanophotonic photoluminescence enhancement.

We illustrate the diverse behavior and the possible scenarios of exciton dynamics using a variety of nanostructures.

First, we analyze how diffusion affects it by spreading excitons out. We study excitonic emitters consisting of orientationally averaged dipoles above an array of silicon nanodisks. Although exciton density and diffusion are 2D because the exciton film is thin, the exciton dipole moment can have components out of the plane—therefore, we average the orientations in all three dimensions.[34] We assume perfect collection efficiency of the emission. We illuminate with a continuous-wave source at low power so that annihilation is initially negligible.

For low diffusion constants, the exciton density concentrates near the edge of the nanodisk, corresponding to the local excitation profile of an electric dipole in the nanodisk (**Figure 2**a). As the non-dimensionalized diffusion constant D' increases, the exciton density distribution expands, eventually becoming uniform over the unit cell. In this case, diffusion suppresses the total photoluminescence enhancement by taking excitons from regions of high radiative enhancement to positions of low enhancement (Figure 2b). The total photoluminescence is a combination of excitation and emission enhancements. Immobile emitters with low intrinsic quantum yield benefit from both excitation and emission enhancements, whereas only the increased excitation is relevant for emitters with high quantum yield.[35,36] The Purcell effect can be strongly modified upon diffusion, while the excitation is unaffected by diffusion in the absence of saturation effects. The impact of diffusion is the strongest for emitters with low quantum yield because of their larger contribution from radiative enhancement. For emitters with high intrinsic quantum yield, the Purcell effect enhances only the decay rate and not the photoluminescence. Diffusion reduces this enhancement (Figure S1a, Supporting Information).

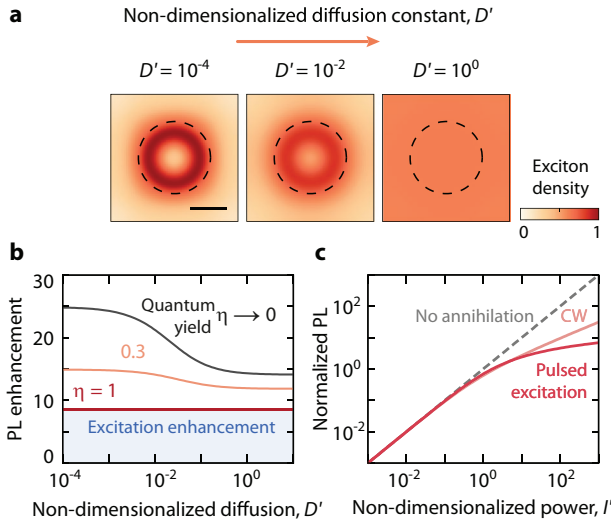

Figure 2. Exciton diffusion and annihilation usually lead to reduced photoluminescence. a) Exciton density of emitters with intrinsic quantum yield $\eta_0 = 1$ above an array of silicon nanodisks with radius $R = 100$, height $H = 75$, and period $P = 365$ nm. A low-power, continuous plane wave is incident from below the disks at $\lambda = 553$ nm. Scale bar 100 nm. b) The nanophotonic photoluminescence enhancement of the nanodisk array decreases due to diffusion. The blue area indicates enhancement due to excitation only. c) In the absence of nanophotonic structures, photoluminescence scales sublinearly with incident power due to annihilation.

In the absence of nanostructures, exciton– exciton annihilation suppresses photoluminescence by opening an additional non-radiative channel at high excitation powers and exciton densities (Figure 2c). Compared to continuous-wave excitation, pulsed excitation creates higher instantaneous exciton densities, thereby reducing emission even further. Nanophotonic structures can ameliorate this deterioration of emission, as we shall discuss later. Additionally, the quick initial decay due to the high exciton density shortens the decay time considerably (Figure S1b, Supporting Information).

2.2. Enhancing Emission Through Diffusion

Generally, the deterioration of nanophotonic enhancement with diffusion is due to losing the advantage of spatial overlap between excitation and emission enhancements. To understand the contribution of each process and their overlap, we solve the non-dimensionalized exciton dynamics Equation (2) analytically for limiting cases of quantum yield, diffusion, and annihilation (Section S1, Supporting Information). We list the photoluminescence enhancement for these extremes in **Table 1** and depict the contributions from excitation and emission and their overlap in Figure 1b, where the levels indicate the increasing role of annihilation. When the incident power is much lower than $I_0 = \Gamma_0 n_0/\sigma$, annihilation is negligible compared to intrinsic decay (bottom level in Figure 1b). In this regime of negligible annihilation ($I' \to 0$) and diffusion length much smaller than the period ($D' \to 0$), the total enhancement for emitters with poor efficiency ($\eta_0 \to 0$) is $\langle F_{ex}(\mathbf{r}) \cdot F_{em}(\mathbf{r}) \rangle$, which is the spatial average of the product of local enhancements in the unit cell. Hence, in the absence of diffusion, we obtain high total enhancement if the excitation and emission significantly overlap.

In the regime of high diffusion, however, the total enhancement becomes $\langle F_{ex}(\mathbf{r}) \rangle \langle F_{em}(\mathbf{r}) \rangle$, which is the product of the average values of excitation and emission in the unit cell. The spatial overlap of the enhancement factors is then no longer of benefit. As a result, the photoluminescence enhancement typically worsens with diffusion for low-efficiency emitters (**Figure 3**a). Although emitters with high quantum yield do not suffer a similar loss of enhancement because their emission efficiency does not change, their decay rate deteriorates

Table 1. Nanophotonic photoluminescence enhancement (F_{tot}) in the presence of exciton dynamics: limiting cases of diffusion, quantum yield, and incident power. $\langle x \rangle$ represents the spatial average of the quantity x in the unit cell. Spatial averages of products of excitation and emission enhancements such as $\langle F_{ex} \cdot F_{em} \rangle$ indicate the benefit of their spatial overlap. Diffusion decouples the enhancements spatially, turning the expressions into products of spatial averages such as $\langle F_{ex} \rangle \langle F_{em} \rangle$.

Diffusion	Quantum yield	Incident power (with annihilation)		
		$I' \to 0$	$I' \to \infty$	
			Continuous	Pulsed
$D' = 0$	$\eta_0 \to 0$	$\langle F_{ex} \cdot F_{em} \rangle$	$\langle \sqrt{F_{ex}} \cdot F_{em} \rangle$	$F_{tot} = \langle F_{em} \rangle$
	$\eta_0 = 1$	$\langle F_{ex} \rangle$	$\langle \sqrt{F_{ex}} \cdot F_{em} \rangle$	$F_{tot} = \langle F_{em} \rangle$
$D' \to \infty$	$\eta_0 \to 0$	$\langle F_{ex} \rangle \langle F_{em} \rangle$	$\langle \sqrt{F_{ex}} \rangle \langle F_{em} \rangle$	$F_{tot} = \langle F_{em} \rangle$
	$\eta_0 = 1$	$\langle F_{ex} \rangle$	$\langle \sqrt{F_{ex}} \rangle \langle F_{em} \rangle$	$F_{tot} = \langle F_{em} \rangle$

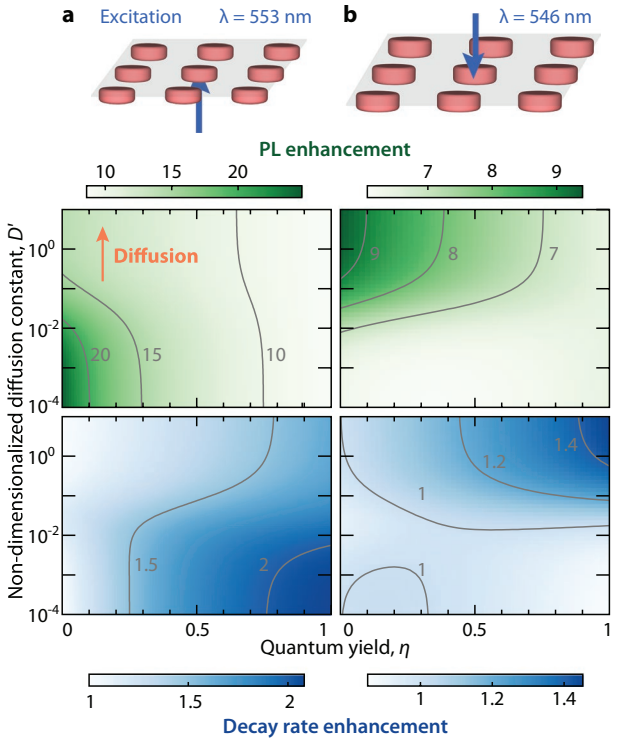

Figure 3. Diffusion can both improve or degrade photoluminescence depending on the nanophotonic system. Photoluminescence and total decay rate enhancements under low-power, pulsed illumination of excitons above arrays of silicon nanodisks: a) illuminated from below with R = 100, H = 75, P = 365 nm; b) illuminated from above with R = 120, H = 90, P = 445 nm. In gray, contours of constant enhancement with their respective values. Excitation and emission wavelengths are equal.

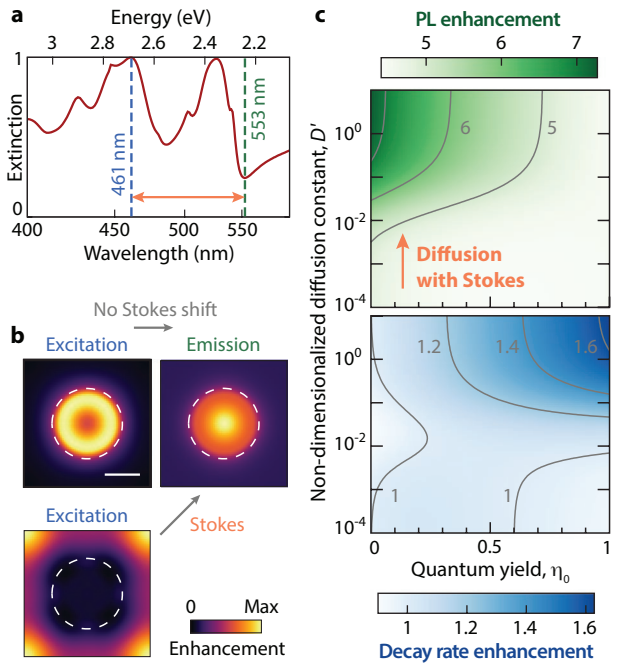

Figure 4. A Stokes shift can decouple excitation and emission enhancements at different wavelengths to improve photoluminescence through diffusion. a) Extinction spectrum of the array of silicon nanodisks in Figure 3a with multiple resonances. b) The maps of excitation and emission enhancements at λ_{em} = 553 nm overlap significantly. Changing the excitation wavelength to 461 nm decouples the excitation enhancement at λ_{ex} from the emission at λ_{em}. Scale bar 100 nm. c) Enhancements of photoluminescence and total decay rate under excitation at λ_{ex} and emission at λ_{em} including the Stokes shift above.

with increasing diffusion (Figure 3a). Surprisingly, diffusion can modify the decay rate of emitters even in the limit of zero quantum yield (Figure S2, Supporting Information).

Diffusion can also improve emission by removing the spatial overlap between enhancement contributions. By controlling the excitation conditions such as the angle of incidence, polarization, or wavelength, we can lift the requirement of spatial overlap for maximum photoluminescence. As a first example, we spatially decouple excitation and emission by exploiting the angular pattern of emission in an array with a different geometry (Figure 3b and Figure S3, Supporting Information). The excitation profile shows a strong front-back asymmetry because the high refractive index of silicon causes retardation of electromagnetic fields along its height.[5] We illuminate the nanodisks from above to benefit from this asymmetry. The photoluminescence increases with diffusion at low η_0, and so does the decay rate enhancement at high η_0. Nanostructures designed under the assumption of immobile emitters can thus behave differently with diffusing excitons. Whether the impact of diffusion on enhancement is beneficial or detrimental depends on the nanophotonic system. Nanostructures aiming at maximum output from excitonic materials should thus take diffusion into account due to their spatially dependent enhancements.[4,7,37,38]

As a second case of enhancement through diffusion, we exploit the Stokes shift between excitation and emission wavelengths to decouple them spatially. We utilize the diversity of resonances supported by arrays of silicon nanodisks (**Figure 4**a). For zero detuning with emission and excitation at $\lambda_{em} = \lambda_{ex}$ = 553 nm, the excitation and radiative enhancements are both strongest above the disk (Figure 4b). The exciton density is highest near the edge because of the relatively high excitation enhancement there (Figure 2a). Due to the spatial overlap between enhancements, diffusion decreases photoluminescence as it transports excitons from regions of high excitation to areas of low radiative enhancements (Figure 3a). However, if the excitonic material has a Stokes shift between excitation at λ_{ex} = 461 and emission at λ_{em} = 553 nm, the excitation enhancement is almost completely decoupled from the emission enhancement (Figure 4b). Diffusion thus takes the excitons generated at λ_{ex} to regions of high radiative enhancement at λ_{em}, improving photoluminescence and decay rate compared to immobile excitons (Figure 4c). Emitters typically have a Stokes shift between excitation and emission, giving us a handle to turn diffusion to our advantage.

2.3. Overcoming Annihilation through Nanophotonic Enhancement

So far, we have only considered the effects of diffusion on nanophotonic enhancement. Next, we add exciton– exciton annihilation, which typically suppresses photoluminescence. As the incident power of a continuous-wave source increases,

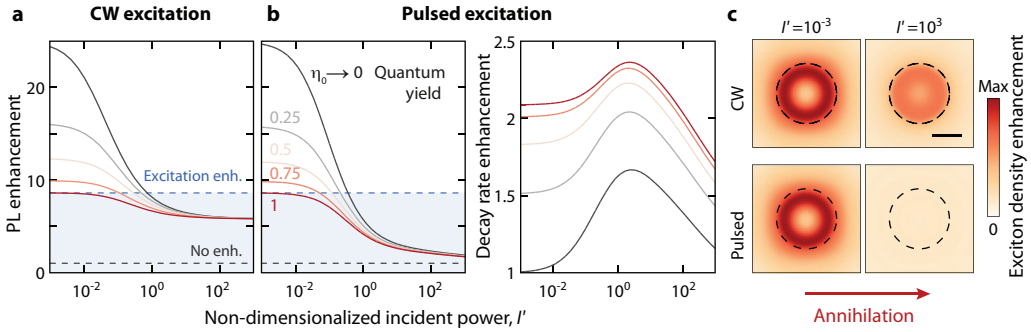

Figure 5. Exciton– exciton annihilation typically suppresses photoluminescence enhancement at increasing excitation powers. a) Photoluminescence enhancement for the array of silicon nanodisks in Figure 3a as a function of incident power under continuous-wave illumination. Blue and gray lines denote the levels of excitation enhancement and no enhancement. b) Enhancement of photoluminescence and total decay rate under pulsed illumination. c) Change in exciton density enhancement averaged over time with increasing incident power.

photoluminescence enhancement usually decreases for all quantum yields in the absence of diffusion (**Figure 5**a for the array in Figure 3a). At high power, the total nanophotonic enhancement falls even below the excitation enhancement (blue line). Exciton– exciton annihilation increases nonlinearly with power, suppressing the effect of excitation enhancement and reducing the steady-state exciton density enhancement (Figure 5c). At low power, the photoluminescence enhancement is due to F_{ex} for high-η_0 emitters, whereas it arises from the product of F_{ex} and F_{em} for low-η_0 emitters. In contrast, at high power, the photoluminescence enhancement is the product of $\sqrt{F_{ex}}$ and F_{em} independent of the quantum yield because exciton– exciton annihilation becomes the dominant non-radiative decay channel (Table 1).

The suppression of photoluminescence is even stronger for pulsed excitation (Figure 5b), where annihilation neutralizes the excitation enhancement completely as manifest in the time-averaged exciton density (Figure 5c). The emission enhancement still results in increased photoluminescence compared to the bare emitters. Exciton density enhancement on the nanostructure modifies the total decay rate via exciton– exciton annihilation, although the effect is neutralized once again at very high incident power (Figure 5b).

Diffusion can alleviate part of the detrimental effects of annihilation by smearing the hotspots of exciton density. Although emitters with high intrinsic quantum yield have diffusion-independent photoluminescence enhancement at low incident power (Figure 4c), the drop in enhancement with increasing power is much slower for highly diffusing excitons (**Figure 6**a).

Next, we demonstrate that it is possible to improve performance even as annihilation becomes dominant. At low incident power, high-η_0 emitters benefit only from excitation enhancement whereas at high power, the effect of excitation diminishes and emission enhancement becomes dominant (Table 1). Therefore, nanophotonic structures with emission enhancement comparable to or higher than excitation enhancement offer improved photoluminescence enhancement with increasing power. This counter-intuitive behavior arises from the increasing benefit of emission enhancement as a strong non-radiative decay channel opens at high exciton densities. We exemplify such a case with an array of silver nanoparticles which has significantly higher emission enhancement compared to excitation enhancement (Figure S4, Supporting Information). Indeed, as the incident power increases, emitters above the array of silver nanoparticles benefit from increasing photoluminescence enhancement (Figure 6b). Although we have shown improved performance here for plasmonic nanoparticles, dielectric nanostructures with strong emission enhancements behave similarly (Figure S5, Supporting Information). High-η_0 emitters with exciton– exciton annihilation are important for light-emitting devices, which suffer from efficiency loss at high powers. The ability to reduce the impact of annihilation on emission through the combination of nanophotonic design and diffusion is thus of practical interest.

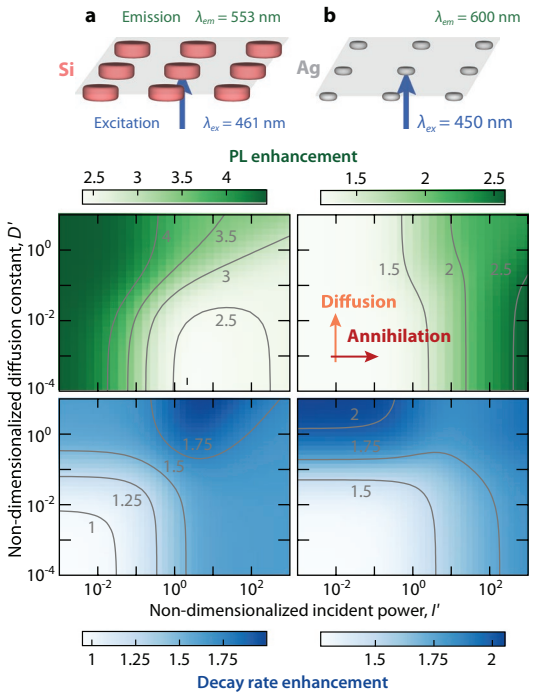

Figure 6. Interplay between nanophotonic properties, annihilation, and diffusion. Increasing incident power can either decrease or increase nanophotonic emission enhancement. a,b) Geometry, photoluminescence enhancement under continuous-wave illumination, and total decay rate enhancement under pulsed illumination, for emitters with $\eta_0 = 1$ above: silicon nanodisks with $R = 100$, $H = 75$, $P = 365$ nm (a); silver nanodisks with $R = 50$, $H = 40$, $P = 350$ nm (b).

2.4. Nanophotonic Enhancement in Relevant Excitonic Materials

Finally, we show that the non-dimensionalized limits of diffusion and annihilation become significant for light emission from realistic excitonic emitters. We tabulate reported excitonic parameters for representative materials and calculate their characteristic exciton density n_0, incident power I_0 and the non-dimensionalized diffusion constant D' (Table S1, Supporting Information). For transition metal dichalcogenide monolayers and 2D perovskites, D' is of the order of unity. As a result, the excitons spread through the entire unit cell before they decay. Monolayer semiconductors with low quantum yield thus benefit from additional enhancement in nanostructures designed for diffusive excitons (Figure S6, Supporting Information). Emitters with high quantum yield also suffer from strong annihilation . The incident power at which annihilation becomes dominant, I_0, is very low (of the order of nW μm^{-2} – μW μm^{-2}), especially for transition metal dichalcogenides (Table S1, Supporting Information). As a result, they benefit from additional enhancement in nanophotonic systems designed for materials with high annihilation (Figure S7, Supporting Information).

Although we focused our analysis on excitons in thin films, the general principles also apply to other geometries. Nanowires support 1D diffusion and can be placed along directions of high excitation and emission enhancements to obtain stronger photoluminescence (Figure S10, Supporting Information). In the case of thick excitonic materials around nanophotonic structures, exciton diffusion will be 3D, and the decay of the evanescent near field away from the nanostructure plane will also play a role. In addition to photonic enhancement, material interfaces can modify intrinsic decay, diffusion, and annihilation through doping, dielectric screening, or phonons.[29,33,39–43] Our model can accommodate such effects through the use of locally varying excitonic parameters modified by the environment. It is also possible to prevent such environmental modification of excitonic parameters with a thin dielectric spacer. At high exciton densities in transition metal dichalcogenide monolayers, exciton– phonon effects modify diffusion, resulting in halo formation.[44–46] Making the diffusion constant dependent on the exciton density[44] in the exciton dynamics equation can model such behavior. Some materials show superdiffusive behavior where the exciton density spreads faster than the prediction from linear diffusion. A rate equation model can describe such behavior by making the diffusion constant dependent on time or exciton density.[47,48] In materials such as organic semiconductors where there are multiple varieties of excitons, incorporating their interconversion into the rate equation can identify effects such as negative diffusion.[49] Additional phenomena could further exploit diffusion to improve performance. Diffusion spreads the excitons away from the nanostructures, where Ohmic losses in the nanophotonic system are stronger. The reduction of absorption losses could therefore further contribute to total enhancement due to diffusion. Analogous to annihilation, saturation effects at higher excitation powers can suppress the enhancement[50] and could be similarly overcome through diffusion. On the other hand, designing nanophotonic systems with extremely high emission enhancements can counteract the effect of diffusion by reducing the lifetime and thus the diffusion length (Figure S9, Supporting Information). Last, applying strain on monolayer semiconductors can result in exciton funneling, the directional transport of excitons toward regions of high strain.[38,51–54] Using nanostructures as sources of both strain and nanophotonic enhancement promises a new direction to control light– matter interaction.

3. Conclusion

We have combined exciton dynamics and nanophotonics to illustrate the range of scenarios beyond the conventional Purcell effect for photoluminescence enhancement in the presence of diffusion and annihilation. Although usually detrimental for light emission, careful nanophotonic design can turn diffusion into an advantage and partly mitigate the detrimental effect of exciton– exciton annihilation. We presented analytical expressions of enhancement for the limiting regimes of diffusion and annihilation to formulate the conditions for improved exciton photoluminescence. Removing the spatial overlap between excitation and emission enhancements can improve emission from diffusive excitons in nanostructured landscapes—for instance, by including a Stokes shift between excitation and emission wavelengths. Similar decoupling is possible through other strategies such as excitation and emission at different angles. It is also possible to alleviate the detrimental effects of exciton– exciton annihilation by tuning the relative strengths of excitation and emission enhancements and by capitalizing on diffusion to reduce the local exciton density. The approach could be extended to electrically generated excitons, which can create highly localized exciton distributions near nanoscale contacts. Additionally, solar cells could benefit from maximizing excitation enhancement near the nanostructures while redistributing the exciton density through diffusion to reduce the loss of excitons through emission and annihilation.

Our results demonstrate the importance of tailoring nanophotonic structures to specific exciton dynamics for maximal performance. As several excitonic materials consist of nano- or microcrystals exhibiting nanophotonic resonances, their photonic properties also have implications for understanding and quantifying exciton dynamics in nanomaterials. The operation principles and limiting regimes that we provide for diffusion and annihilation in nanophotonic landscapes can thus guide the design of efficient and high-power devices. Our findings apply to light-emitting diodes or lasers using relevant families of semiconductors in the form of nanoparticles, nanowires, thin films, or monolayers.

4. Experimental Section

Electromagnetic Simulations: The electromagnetic simulations were performed using the SIE method for periodic nanostructures.[55,56] The permittivities of silicon and silver from Green[57] and Johnson and Christy were used.[58] A homogeneous relative permittivity $\varepsilon_r = 1.5$ was set for the background medium as the geometric mean of air and glass to approximate the effect of a substrate. A realistic rounding radius of 20 nm to the sharp edges of the nanodisks was applied.

The emitters were treated as electric dipole sources lying on a plane 5 nm above the nanodisks. To compute the excitation enhancement F_{ex}, the system was illuminated with a plane wave under normal incidence from above or below depending on optimal excitation conditions and

the electric field **E** on the plane above the nanostructure was evaluated. The excitation enhancement for dipolar emitters orientationally averaged in three dimensions is $|\mathbf{E}|^2/|\mathbf{E}_0|^2$, where $\mathbf{E}_0$ is the electric field in the absence of the nanostructures.

The emission enhancement F_{em} is the integral of the power radiated in all directions (θ, ϕ), normalized to the same quantity in the absence of nanostructures. The dipole radiation was computed in a given direction (θ, ϕ) using electromagnetic reciprocity[59] by evaluating the field intensity at the location of the emitter under illumination by a plane wave incident from the same direction.[60–62] This method assumed no absorption losses in the nanodisks that might reduce antenna radiation efficiency. The emission enhancement of a dipole depends on its orientation. The average emission enhancements for emitters were computed along all possible orientations in three dimensions, integrating total photoluminescence in all directions.

For emitters such as transition metal dichalcogenides where the dipoles are oriented in the plane, excitation enhancement required using the in-plane projection of the electric field. Additionally, orientational averaging should then be performed in two dimensions. With these modifications, our treatment applies to 2D excitonic materials as well and does not change the results qualitatively (Figure S8, Supporting Information).

Numerical Solution of Exciton Dynamics: To solve the non-dimensionalized exciton dynamics Equation (2) numerically, the exciton density was discretized into a grid with non-dimensionalized coordinates: $n'(x'_i, y'_j)$ where $x'_i = i/2N, y'_j = j/2N$ for $(i, j) \in \{-N, \ldots N\}$. The value of N was chosen in each simulation to obtain 5 nm spatial resolution. As a result of periodicity, the exciton densities were equal at opposite edges of the unit cell (indices $-N$ and N). In the limiting case of low incident power, the quadratic annihilation term vanishes resulting in a linear differential equation in n'. Under continuous-wave illumination, in the steady state, $[F_{decay} - D'\nabla'^2]n' = F_{ex}I'$, where the explicit spatial dependence was dropped. Taking the spatial Fourier transform

$$\left[\tilde{F}_{decay} \circledast + D' q'^2\right]\tilde{n}' = \tilde{F}_{ex} I' \tag{3}$$

where the quantities with a tilde (such as $\tilde{n}'$) are Fourier transforms of the real-space quantities, $\tilde{F}_{decay} \circledast$ is the circular convolution matrix for $\tilde{F}_{decay}$, and the matrix q'^2 is the squared momentum in the Fourier transform of the discrete Laplace operator, with elements $q'^2_{l,m} = 4\pi^2(l^2 + m^2)$. Inverting the matrix on the left-hand side of Equation (3) gives the steady-state exciton density. Its eigenvalues describe the time evolution under pulsed illumination, providing the total decay rate enhancement.

In the presence of annihilation, linear methods cannot be used any longer. Hence the system was left to evolve explicitly according to Equation (2) using the forward Euler method until $T = 10\tau_0$. Under continuous-wave illumination, the system reached a steady state by this time. Pulsed excitation was modeled using an ultrashort impulse $I'\delta(t')$ so that the exciton density instantaneously becomes $n'(\mathbf{r}', 0) = F_{ex}(\mathbf{r}')I'$. It was ensured that the high initial decay rates do not result in numerical errors by using an adaptive time step that limited the maximum relative change in exciton density at a location within a time step to one percent. The total photoluminescence from the unit cell is then

$$PL = \eta_0 \int\int\int n'(\mathbf{r}', t') F_{em}(\mathbf{r}')\, dt'\, d\mathbf{r}'^2 \tag{4}$$

The decay time can also be calculated as the mean lifetime of emission from the temporal decay of photoluminescence

$$\tau = \frac{\eta_0 \int\int\int n'(\mathbf{r}', t') F_{em}(\mathbf{r}') t'\, dt'\, d\mathbf{r}'^2}{PL} \tag{5}$$

The total decay rate enhancement is the ratio of the decay time without the nanostructure to the average decay time in the presence of the nanostructure.

Supporting Information

Supporting Information is available from the Wiley Online Library or from the author.

Acknowledgements

The authors thank Rasmus H. Godiksen for illuminating discussions. This work was financially supported by the Netherlands Organization for Scientific Research (NWO) through Gravitation grant "Research Centre for Integrated Nanophotonics" (024.002.033), START-UP grant (740.018.009), and Innovational Research Incentives Scheme (VICI Grant no. 680-47-628). S.W. was supported by Priority Academic Program Development (PAPD) of Jiangsu Higher Education Institutions. Simulations in this work were carried out on the Dutch national e-infrastructure with the support of SURF Cooperative.

Conflict of Interest

The authors declare no conflict of interest.

Data Availability Statement

The data that support the findings of this study are available from the corresponding author upon reasonable request.

Keywords

exciton transport, exciton–exciton annihilation, Mie resonances, nanoparticle arrays, plasmonic resonances, Purcell effect

Received: January 16, 2022
Revised: April 10, 2022
Published online: June 7, 2022

[1] S. Bidault, M. Mivelle, N. Bonod, *J. Appl. Phys.* **2019**, *126*, 094104.
[2] E. Y. Tiguntseva, G. P. Zograf, F. E. Komissarenko, D. A. Zuev, A. A. Zakhidov, S. V. Makarov, Y. S. Kivshar, *Nano Lett.* **2018**, *18*, 1185.
[3] V. Rutckaia, F. Heyroth, A. Novikov, M. Shaleev, M. Petrov, J. Schilling, *Nano Lett.* **2017**, *17*, 6886.
[4] T. Bucher, A. Vaskin, R. Mupparapu, F. J. F. Löchner, A. George, K. E. Chong, S. Fasold, C. Neumann, D.-Y. Choi, F. Eilenberger, F. Setzpfandt, Y. S. Kivshar, T. Pertsch, A. Turchanin, I. Staude, *ACS Photonics* **2019**, *6*, 1002.
[5] T. V. Raziman, R. H. Godiksen, M. A. Müller, A. G. Curto, *ACS Photonics* **2019**, *6*, 2583.
[6] S. Murai, G. W. Castellanos, T. V. Raziman, A. G. Curto, J. Rivas, *Adv. Opt. Mater.* **2020**, *8*, 1902024.
[7] A. F. Cihan, A. G. Curto, S. Raza, P. G. Kik, M. L. Brongersma, *Nat. Photon.* **2018**, *12*, 284.
[8] J. N. Farahani, D. W. Pohl, H.-J. Eisler, B. Hecht, *Phys. Rev. Lett.* **2005**, *95*, 017402.
[9] P. Anger, P. Bharadwaj, L. Novotny, *Phys. Rev. Lett.* **2006**, *96*, 113002.
[10] S. Kühn, U. Håkanson, L. Rogobete, V. Sandoghdar, *Phys. Rev. Lett.* **2006**, *97*, 017402.
[11] G. Vecchi, V. Giannini, J. Gómez Rivas, *Phys. Rev. Lett.* **2009**, *102*, 146807.
[12] A. G. Curto, G. Volpe, T. H. Taminiau, M. P. Kreuzer, R. Quidant, N. F. van Hulst, *Science* **2010**, *329*, 930.
[13] K. C. Y. Huang, M.-K. Seo, Y. Huo, T. Sarmiento, J. S. Harris, M. L. Brongersma, *Nat. Commun.* **2012**, *3*, 1005.
[14] A. Mohammadi, V. Sandoghdar, M. Agio, *New J. Phys.* **2008**, *10*, 105015.
[15] L. Novotny, B. Hecht, *Principles of Nano-Optics*, 2nd ed., Cambridge University Press, Cambridge **2012**.

[16] S. D. Stranks, G. E. Eperon, G. Grancini, C. Menelaou, M. J. P. Alcocer, T. Leijtens, L. M. Herz, A. Petrozza, H. J. Snaith, *Science* **2013**, *342*, 341.
[17] E.-P. Yao, B. J. Bohn, Y. Tong, H. Huang, L. Polavarapu, J. Feldmann, *Adv. Opt. Mater.* **2019**, *7*, 1801776.
[18] S. Deng, E. Shi, L. Yuan, L. Jin, L. Dou, L. Huang, *Nat. Commun.* **2020**, *11*, 664.
[19] N. Kumar, Q. Cui, F. Ceballos, D. He, Y. Wang, H. Zhao, *Nanoscale* **2014**, *6*, 4915.
[20] L. Yuan, T. Wang, T. Zhu, M. Zhou, L. Huang, *J. Phys. Chem. Lett.* **2017**, *8*, 3371.
[21] G. M. Akselrod, F. Prins, L. V. Poulikakos, E. M. Y. Lee, M. C. Weidman, A. J. Mork, A. P. Willard, V. Bulović, W. A. Tisdale, *Nano Lett.* **2014**, *14*, 3556.
[22] E. M. Y. Lee, W. A. Tisdale, *J. Phys. Chem. C* **2015**, *119*, 9005.
[23] O. V. Mikhnenko, P. W. M. Blom, T.-Q. Nguyen, *Energy Environ. Sci.* **2015**, *8*, 1867.
[24] L. Cognet, D. A. Tsyboulski, J.-D. R. Rocha, C. D. Doyle, J. M. Tour, R. B. Weisman, *Science* **2007**, *316*, 1465.
[25] A. R. Amori, Z. Hou, T. D. Krauss, *Annu. Rev. Phys. Chem.* **2018**, *69*, 81.
[26] T. Hertel, S. Himmelein, T. Ackermann, D. Stich, J. Crochet, *ACS Nano* **2010**, *4*, 7161.
[27] W. Li, S. K. Yadavalli, D. Lizarazo-Ferro, M. Chen, Y. Zhou, N. P. Padture, R. Zia, *ACS Energy Lett.* **2018**, *3*, 2669.
[28] J. M. Snaider, Z. Guo, T. Wang, M. Yang, L. Yuan, K. Zhu, L. Huang, *ACS Energy Lett.* **2018**, *3*, 1402.
[29] A. J. Goodman, D.-H. Lien, G. H. Ahn, L. L. Spiegel, M. Amani, A. P. Willard, A. Javey, W. A. Tisdale, *J. Phys. Chem. C* **2020**, *124*, 12175.
[30] L. Yuan, L. Huang, *Nanoscale* **2015**, *7*, 7402.
[31] D. Sun, Y. Rao, G. A. Reider, G. Chen, Y. You, L. Brézin, A. R. Harutyunyan, T. F. Heinz, *Nano Lett.* **2014**, *14*, 5625.
[32] S. Mouri, Y. Miyauchi, M. Toh, W. Zhao, G. Eda, K. Matsuda, *Phys. Rev. B* **2014**, *90*, 155449.
[33] Y. Yu, Y. Yu, C. Xu, A. Barrette, K. Gundogdu, L. Cao, *Phys. Rev. B* **2016**, *93*, 201111.
[34] T. V. Raziman, O. J. F. Martin, *J. Phys. Chem. C* **2016**, *120*, 21037.
[35] G. Sun, J. B. Khurgin, R. A. Soref, *Appl. Phys. Lett.* **2009**, *94*, 101103.
[36] A. Kinkhabwala, Z. Yu, S. Fan, Y. Avlasevich, K. Müllen, W. E. Moerner, *Nat. Photonics* **2009**, *3*, 654.
[37] O. Mey, F. Wall, L. M. Schneider, D. Günder, F. Walla, A. Soltani, H. Roskos, N. Yao, P. Qing, W. Fang, A. Rahimi-Iman, *ACS Nano* **2019**, *13*, 5259.
[38] L. Sortino, P. G. Zotev, S. Mignuzzi, J. Cambiasso, D. Schmidt, A. Genco, M. Aßmann, M. Bayer, S. A. Maier, R. Sapienza, A. I. Tartakovskii, *Nat. Commun.* **2019**, *10*, 5119.
[39] Y. Hoshi, T. Kuroda, M. Okada, R. Moriya, S. Masubuchi, K. Watanabe, T. Taniguchi, R. Kitaura, T. Machida, *Phys. Rev. B* **2017**, *95*, 241403.
[40] L. M. Schneider, S. Lippert, J. Kuhnert, O. Ajayi, D. Renaud, S. Firoozabadi, Q. Ngo, R. Guo, Y. D. Kim, W. Heimbrodt, J. C. Hone, A. Rahimi-Iman, *Nano-Struct. Nano-Objects* **2018**, *15*, 84.
[41] Y. Fu, D. He, J. He, A. Bian, L. Zhang, S. Liu, Y. Wang, H. Zhao, *Adv. Mater. Interfaces* **2019**, *6*, 1901307.
[42] D. Rhodes, S. H. Chae, R. Ribeiro-Palau, J. Hone, *Nat. Mater.* **2019**, *18*, 541.
[43] R. H. Godiksen, S. Wang, T. V. Raziman, M. H. D. Guimaraes, J. G. Rivas, A. G. Curto, *Nano Lett.* **2020**, *20*, 4829.
[44] M. Kulig, J. Zipfel, P. Nagler, S. Blanter, C. Schüller, T. Korn, N. Paradiso, M. M. Glazov, A. Chernikov, *Phys. Rev. Lett.* **2018**, *120*, 207401.
[45] M. M. Glazov, *Phys. Rev. B* **2019**, *100*, 045426.
[46] R. Perea-Causín, S. Brem, R. Rosati, R. Jago, M. Kulig, J. D. Ziegler, J. Zipfel, A. Chernikov, E. Malic, *Nano Lett.* **2019**, *19*, 7317.
[47] E. Najafi, V. Ivanov, A. Zewail, M. Bernardi, *Nat. Commun.* **2017**, *8*, 15177.
[48] E. G. Flekkøy, A. Hansen, B. Baldelli, *Front. Phys.* **2021**, *9*, 640560.
[49] A. M. Berghuis, T. V. Raziman, A. Halpin, S. Wang, A. G. Curto, J. G. Rivas, *J. Phys. Chem. Lett.* **2021**, *12*, 1360.
[50] A. M. Kern, A. J. Meixner, O. J. F. Martin, *ACS Nano* **2012**, *6*, 9828.
[51] A. Castellanos-Gomez, R. Roldán, E. Cappelluti, M. Buscema, F. Guinea, H. S. J. van der Zant, G. A. Steele, *Nano Lett.* **2013**, *13*, 5361.
[52] X. Liu, W. Guo, *Phys. Rev. B* **2019**, *99*, 035401.
[53] H. Moon, G. Grosso, C. Chakraborty, C. Peng, T. Taniguchi, K. Watanabe, D. Englund *arXiv:1906.10077 [cond-mat]*, 2019.
[54] L. Sortino, M. Brooks, P. G. Zotev, A. Genco, J. Cambiasso, S. Mignuzzi, S. A. Maier, G. Burkard, R. Sapienza, A. I. Tartakovskii, *ACS Photonics* **2020**, *7*, 2413.
[55] B. Gallinet, A. M. Kern, O. J. F. Martin, *J. Opt. Soc. Am. A* **2010**, *27*, 2261.
[56] T. V. Raziman, W. R. C. Somerville, O. J. F. Martin, E. C. Le Ru, *J. Opt. Soc. Am. B* **2015**, *32*, 485.
[57] M. A. Green, *Sol. Energy Mater. Sol. Cells* **2008**, *92*, 1305.
[58] P. B. Johnson, R. W. Christy, *Phys. Rev. B* **1972**, *6*, 4370.
[59] W. C. Chew, *Waves and Fields in Inhomogeneous Media*, Van Nostrand Reinhold **1990**.
[60] N. Anttu, *J. Appl. Phys.* **2016**, *120*, 043108.
[61] P. Kivisaari, Y. Chen, N. Anttu, *Nano Futures* **2018**, *2*, 015001.
[62] A. Vaskin, J. Bohn, K. E. Chong, T. Bucher, M. Zilk, D. Choi, D. N. Neshev, Y. S. Kivshar, T. Pertsch, I. Staude, *ACS Photonics* **2018**, *5*, 1359.